

Thin-film transistors based on p-type Cu_2O thin films produced at room temperature

Elvira Fortunato, Vitor Figueiredo, Pedro Barquinha, Elangovan Elamurugu, Raquel Barros, Gonalo Gonalves, Sang-Hee Ko Park, Chi-Sun Hwang, and Rodrigo Martins

Citation: *Appl. Phys. Lett.* **96**, 192102 (2010); doi: 10.1063/1.3428434

View online: <http://dx.doi.org/10.1063/1.3428434>

View Table of Contents: <http://aip.scitation.org/toc/apl/96/19>

Published by the [American Institute of Physics](#)

Articles you may be interested in

[p-channel thin-film transistor using p-type oxide semiconductor, SnO](#)
Applied Physics Letters **93**, 032113 (2008); 10.1063/1.2964197

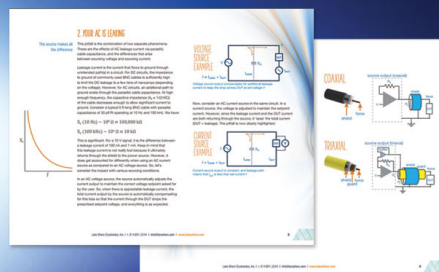
[Epitaxial growth of high mobility \$\text{Cu}_2\text{O}\$ thin films and application to p-channel thin film transistor](#)
Applied Physics Letters **93**, 202107 (2008); 10.1063/1.3026539

[Transparent p-type \$\text{SnO}_x\$ thin film transistors produced by reactive rf magnetron sputtering followed by low temperature annealing](#)
Applied Physics Letters **97**, 052105 (2010); 10.1063/1.3469939

[Fabrication of p-channel thin-film transistors using CuO active layers deposited at low temperature](#)
Applied Physics Letters **97**, 222109 (2010); 10.1063/1.3521310

[Sputtering formation of p-type SnO thin-film transistors on glass toward oxide complimentary circuits](#)
Applied Physics Letters **97**, 072111 (2010); 10.1063/1.3478213

[p-channel thin-film transistors based on spray-coated \$\text{Cu}_2\text{O}\$ films](#)
Applied Physics Letters **102**, 163505 (2013); 10.1063/1.4803085



5 Electronic Measurement Pitfalls to Avoid

Get the whitepaper

Thin-film transistors based on p-type Cu_2O thin films produced at room temperature

Elvira Fortunato,^{1,a)} Vitor Figueiredo,¹ Pedro Barquinha,¹ Elangovan Elamurugu,¹ Raquel Barros,^{1,2} Gonalo Gonalves,¹ Sang-Hee Ko Park,³ Chi-Sun Hwang,³ and Rodrigo Martins¹

¹Departamento de Ci4ncia dos Materiais, CENIMAT/13N, Faculdade de Ci4ncias e Tecnologia, FCT, Universidade Nova de Lisboa and CEMOP-UNINOVA, 2829-516 Caparica, Portugal

²Materiais Avanados, INNOVNANO, SA, 7600-095 Aljustrel, Portugal

³Electronic and Telecommunications Research Institute, 138 Gajeongro, Yuseong-gu, Daejeon, 305-700, Republic of Korea

(Received 21 March 2010; accepted 18 April 2010; published online 10 May 2010)

Copper oxide (Cu_2O) thin films were used to produce bottom gate p-type transparent thin-film transistors (TFTs). Cu_2O was deposited by reactive rf magnetron sputtering at room temperature and the films exhibit a polycrystalline structure with a strongest orientation along (111) plane. The TFTs exhibit improved electrical performance such as a field-effect mobility of $3.9 \text{ cm}^2/\text{V s}$ and an on/off ratio of 2×10^2 . © 2010 American Institute of Physics. [doi:10.1063/1.3428434]

Solid state devices based on cuprous oxide (Cu_2O) semiconductors are known for more than 80 years even before the era of Si devices. Rectifier diodes based on this semiconductor were used industrially as early as 1926 (Ref. 1) and most of the theory of semiconductors was developed based on Cu_2O devices.^{2–4} Besides that, Cu_2O was regarded as one of the most promising materials for application in solar cells^{5–7} due to its high-absorption coefficient in the visible region, nontoxicity, abundant availability, and low-cost production.⁸ Cu_2O has a cubic structure with a direct band gap of 2.1 eV (Ref. 9) and shows p-type conductivity (σ) with hole mobility (μ_H) exceeding $100 \text{ cm}^2/\text{V s}$.¹⁰ The p-type character of Cu_2O is attributed to the presence of negatively charged copper vacancies (V_{Cu}), which introduce an acceptor level about 0.3 eV above the valence band (V_B).¹¹ It was also proposed by some authors the coexistence of both acceptor and donor intrinsic levels with a ratio slightly larger than 1 and less than 10.^{12,13} The nature of the donor levels is not completely clear being even controversial where the simplest candidates are oxygen vacancies.¹⁴ In contrast to the majority of metal oxides, in which the top of V_B is mainly formed from localized and anisotropic O $2p$ orbitals, here leads to a low hole mobility due to hopping conduction, here the top of the V_B is composed of fully occupied hybridized orbitals (Cu $3d^{10}$ and O $2p$) with Cu d sates dominating the top of the V_B . Figure 1(a) illustrates the chemical bond between an oxide ion and a cation that has a closed-shell electronic configuration. Figure 1(b) shows a pictorial representation of the more

important defects in Cu_2O and Fig. 1(c) reveals the simple electronic model proposed by Brattain,¹² consisting of a compensated semiconductor with one acceptor level at 0.3 eV and a deep donor level at 0.9 eV from V_B .

The development of p-n junctions and p-type thin-film transistors (TFTs) is a major goal, as this would lead to the fabrication of complementary metal oxide semiconductor (CMOS) structures where both n- and p-type transistors are needed. The interest in this field was renewed in 1997 when Kawazoe *et al.*¹⁵ reported p-type conductivity in a highly transparent thin film of copper aluminum oxide.

Despite the fact that high quality p-type Cu-based oxide semiconductor thin films have already been achieved,^{10,16–18} so far there is only one report on p-type Cu_2O TFTs (Ref. 18) but without satisfactory requirements for practical applications.

In this work, we report p-type Cu_2O TFTs deposited by reactive rf magnetron sputtering at room temperature (RT), with the final devices requiring annealing temperatures of only 200 °C.

Cu_2O films were grown by reactive rf magnetron sputtering at RT in a homemade system. A 2" diameter Cu metal target (with 99.997% purity) was used at 15 cm from the substrate (soda-lime glass), at a base pressure of 3.4×10^{-4} Pa. The deposition pressure ($P_{\text{Ar}}+P_{\text{O}_2}$) and the rf power were 0.6 Pa and 50 W, respectively. To evaluate the optimal growing conditions for p-type Cu_2O films, the oxygen partial pressure ($O_{\text{PP}}=P_{\text{O}_2}/P_{\text{Ar}}+P_{\text{O}_2}$) was varied be-

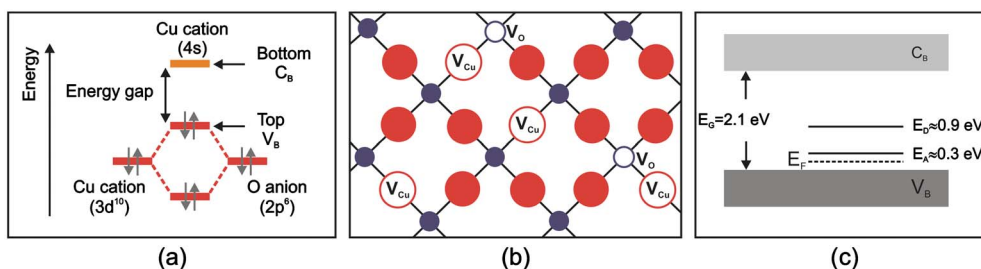


FIG. 1. (Color online) (a) Chemical bond between an oxide ion and a cation that has a closed-shell electronic configuration; (b) a pictorial representation of the more important defects in Cu_2O ; and (c) a simple electronic model proposed by Brattain, with a compensated semiconductor with one acceptor level at 0.3 eV and a deep donor level at 0.9 eV from V_B .

^{a)} Author to whom correspondence should be addressed. Electronic mail: elvira.fortunato@fct.unl.pt. Tel.: +351 212948562. FAX: +351 212948558.

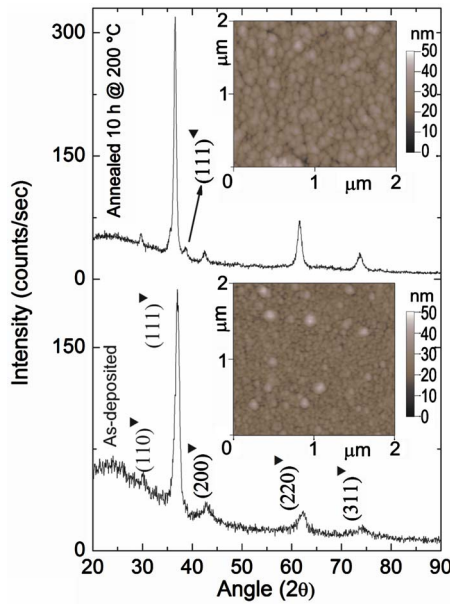


FIG. 2. (Color online) X-ray pattern of the Cu_2O film annealed at 200°C in air for 10 h in comparison with the as-deposited film. (Symbol representations: \blacktriangledown — Cu_2O phase and \blacktriangleleft — CuO phase.) The insets show the AFM images of the corresponding films.

tween 0% and 100%, fixing the film thickness at 200 nm, measured with a surface profilometer. The films' structure was analyzed by x-ray diffraction (XRD) experiments in grazing incidence geometry using $\text{Cu } K_{\alpha 1,2}$ lines. The optical transmittance measurements were performed with a double beam spectrophotometer in the wavelength from 200 to 2500 nm. Atomic force microscopy (AFM) was done in order to investigate the surface topology, operated in ac mode. Electrical transport properties were examined by Hall Effect and σ measurements as a function of absolute temperature (T) using samples with the van der Pauw and planar gap configurations, respectively.

Bottom-gate TFTs were fabricated using 40 nm thick Cu_2O thin films as semiconductors. For the gate dielectric an engineered insulator consisting of a superlattice of Al_2O_3 and TiO_2 (ATO)¹⁹ with a thickness of 220 nm deposited on a glass coated with a 200 nm thick indium tin oxide (ITO) film used as the gate electrode. The source-drain electrodes consist of an indium zinc oxide (IZO) film with 250 nm produced by rf magnetron sputtering at RT.^{20,21} Both the semiconductor and the source-drain electrodes were patterned by lift-off yielding TFTs with a width-to-length ratio (W/L) of 3.3, with $L=15 \mu\text{m}$. The final devices were annealed at 200°C for 1, 5, and 10 h in air using a tubular furnace and the electrical characterization was performed with an Agilent 4155C semiconductor parameter analyzer and a Cascade Microtech M150 microprobe station inside a dark box at ambient atmosphere.

Typical XRD patterns obtained from films annealed for 10 h is comparatively shown in Fig. 2 with the one of as-deposited films. It is found that the annealing is not effective in inducing any change in the Cu_2O phase. However, the increasing intensity of the strongest orientation along (111) with the increase in annealing time has confirmed the improvement in crystallinity of the as-deposited films. The grain size (d_g) inferred from Scherrer formula²² for as-deposited films is 8.30 nm, increasing with the annealing time to a maximum of 15.72 nm for films annealed for 10 h.

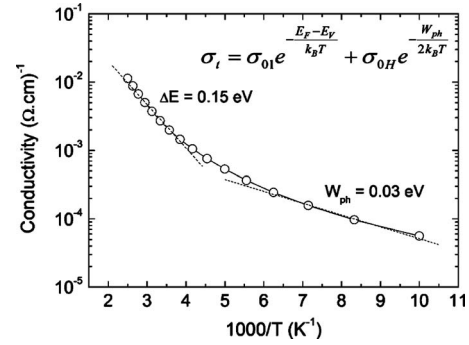


FIG. 3. Temperature dependence of dark conductivity for a Cu_2O thin film with 270 nm. The equation represents the conduction mechanisms for this type of semiconductors. For higher temperatures the conductivity is controlled by an acceptor center located 0.3 eV above the top of V_B (V_{Cu}) while for low temperatures the conductivity is controlled by hopping.

To substantiate the increase in d_g the films were analyzed by AFM and the obtained microstructures are shown as an inset in Fig. 2. The surface roughness increased from 4.6 to 10.4 nm corroborating the d_g obtained from XRD data.

The dependence of σ on T is shown in Fig. 3 for the films produced with 9% O_{pp} . These films exhibit the Cu_2O phase and typical semiconductor behavior. From the experimental data we notice that $\sigma(T)$ data are fitted by two conduction paths controlled, respectively, by an acceptor energy level E_A and by phonons of energy W_{ph} to which activation energies of about 0.15 eV and 0.03 eV are, respectively, associated. Taking into account the equation inside Fig. 3,²³ where the Fermi energy level (E_F) is assumed to be around the middle of energy gap between E_A and the top energy of V_B , we estimate $E_A \approx 2\Delta E \approx 2(E_F - E_V) \approx 0.30$ eV and $W_{\text{ph}} \approx 0.06$ eV, which is in agreement with the conduction path model proposed by other authors.^{12,23–25} A p-type resistivity (ρ) of $2.7 \times 10^3 \Omega \text{cm}$, $\mu_H \approx 0.65 \text{ cm}^2/\text{Vs}$ and a carrier concentration (N) of $3.7 \times 10^{15} \text{ cm}^{-3}$ were obtained at RT. The p-type conduction was also confirmed by Seebeck measurements performed in the same sample. After annealing at 200°C for 10 h, ρ and μ_H increase to $1 \times 10^4 \Omega \text{cm}$ and $18.5 \text{ cm}^2/\text{Vs}$, respectively, while N decreases to values around $3 \times 10^{13} \text{ cm}^{-3}$.

The optical transmittance spectrum through the entire Cu_2O -TFT in the wavelength range between 200 and 2500 nm is shown in Fig. 4. The average optical transmission in the visible part of the spectrum is 80% while at 550 nm (maximum sensitivity for the human eye) is 85%, which in-

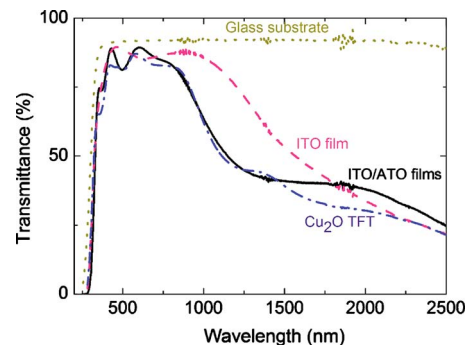


FIG. 4. (Color online) Optical transmission spectra for the entire Cu_2O -TFT structure including the glass substrate; it is possible to observe that the Cu_2O -TFT is fully transparent to visible light. For comparison purposes, the optical transmission spectra for the glass substrate, the ITO, and the ITO/ATO films are also presented.

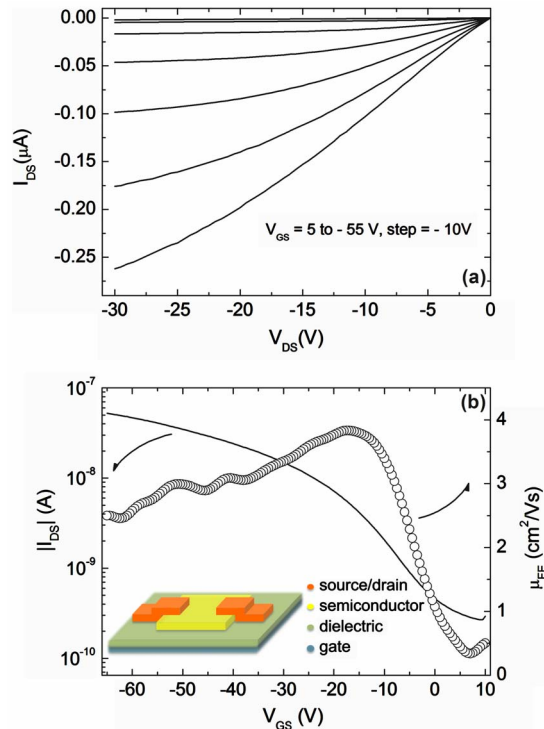


FIG. 5. (Color online) (a) Output characteristics (I_{DS} - V_{DS}); (b) Transfer characteristics ($|I_{DS}$ - V_{GS}) at $V_D = -5$ V (left axis) and μ_{FE} as a function of V_{GS} (right axis), for a typical Cu_2O TFT produced at RT and annealed in air at 200 °C. The inset shows the structure of the bottom gate TFT.

indicates that transmission losses due to the Cu_2O -TFTs are negligible (7%) when compared to the uncoated glass substrate. The lower transmittance at the near infrared region is associated to the large N of the ITO and IZO films which shifts the infrared absorption edge toward the visible, being this shift determined by the plasma oscillation of the free carriers.²⁶ The optical band gap (E_{op}) for direct allowed transitions of the Cu_2O thin films was calculated using Tauc's law as follows: $\alpha^2 = (h\nu - E_{op})$, where α represents the absorption coefficient, h the Planck's constant, and ν the photon frequency. The obtained value was 2.39 eV, which is slightly higher than the conventional value of 2.1 eV for Cu_2O .²⁷

Figure 5(a) shows the output characteristics of a p-type Cu_2O TFT. The drain-to-source voltage (V_{DS}) is swept from +10 to -60 V and the gate-to-source voltage (V_{GS}) is stepped between +5 and -55 V. The output characteristics of the device shows clear linear and saturation regions and does not present significant current crowding for low V_{DS} , indicating low series resistance in source-drain contacts. Figure 5(b) shows the transfer characteristics with $V_{DS} = -5$ V for the same device presented in Fig. 5(a). V_{GS} is swept between -60 to +10 V.

The on/off ratio is 2×10^2 , the peak value of the field-effect mobility (μ_{FE} , calculated by the transconductance in the linear regime) is around $3.9 \text{ cm}^2/\text{V s}$, while the V_T is -12.0 V. The transfer curve presents some nonlinearity, which is reflected in a peculiar behavior of the $\mu_{FE} - V_G$, mainly for high V_G . This could be related with trap filling processes arising, for instance, from a nonoptimized dielectric/semiconductor interface, which should be improved in the future. The inset in Fig. 5(b) shows the structure of the bottom gate TFT.

We have demonstrated the possibility to produce p-type transparent Cu_2O semiconductors by RT reactive magnetron sputtering, followed by annealing treatment at 200 °C. The Cu_2O films are polycrystalline with a strong orientation along the (111) plane. After annealing in air at 200 °C for 10 h, we improve μ_H from 0.65 to $18.5 \text{ cm}^2/\text{V s}$, which is associated to an increase in the grain size, from 8.30 to 15.72 nm. Concerning the optical properties, the p-type films present $E_{op} \approx 2.34 \text{ eV}$ and the films have an average transmittance around 85%, between 400 and 2000 nm for a thickness of 40 nm. Bottom gate p-type Cu_2O TFTs present a $\mu_{FE} \approx 3.9 \text{ cm}^2/\text{V s}$, an on/off ratio of 2×10^2 and a V_T of -12.0 V. The low temperature process together with the good electrical performance of the devices at this early research stage will contribute for the optimization of p-type oxide-based devices and for their integration in CMOS structures allowing their use in flexible, low cost and transparent electronic circuits.

This work was funded by the Portuguese Science Foundation (FCT-MCTES) through projects PTDC/CTM/73943/2006, PTDC/EEA-ELC/64975/2006, ERC 2008 Advanced Grant (INVISIBLE Contract No. 228144) and IT R&D program of MKE (Contract No. 2006-S079-03, Smart window with transparent electronic devices) from ETRI Korea. We thank K. Nomura for the Seebeck measurements and N. Franco for the XRD analysis.

¹L. O. Grondahl, *Science* **64**, 306 (1926).

²E. Duhme and W. Schottky, *Naturwiss.* **18**, 735 (1930).

³W. Schottky and F. Waibel, *Phys. Z.* **34**, 858 (1933).

⁴W. Schottky and F. Waibel, *Phys. Z.* **36**, 912 (1935).

⁵C. Wadia, A. P. Alivisatos, and D. M. Kammen, *Environ. Sci. Technol.* **43**, 2072 (2009).

⁶R. J. Iwanowski and D. Trivich, *Sol. Cells* **13**, 253 (1985).

⁷L. C. Olsen, R. C. Bohara, and M. W. Urie, *Appl. Phys. Lett.* **34**, 47 (1979).

⁸V. Figueiredo, E. Elangovan, G. Goncalves, P. Barquinha, L. Pereira, N. Franco, E. Alves, R. Martins, and E. Fortunato, *Appl. Surf. Sci.* **254**, 3949 (2008).

⁹M. A. Rafea and N. Roushdy, *J. Phys. D: Appl. Phys.* **42**, 015413 (2009).

¹⁰B. S. Li, K. Akimoto, and A. Shen, *J. Cryst. Growth* **311**, 1102 (2009).

¹¹H. Raebiger, S. Lany, and A. Zunger, *Phys. Rev. B* **76**, 045209 (2007).

¹²W. H. Brattain, *Rev. Mod. Phys.* **23**, 203 (1951).

¹³G. P. Pollack and D. Trivich, *J. Appl. Phys.* **46**, 163 (1975).

¹⁴O. Porat and I. Riess, *Solid State Ionics* **81**, 29 (1995).

¹⁵H. Kawazoe, M. Yasukawa, H. Hyodo, M. Kurita, H. Yanagi, and H. Hosono, *Nature (London)* **389**, 939 (1997).

¹⁶M. Ivill, M. E. Overberg, C. R. Abernathy, D. P. Norton, A. F. Hebard, N. Theodoropoulou, and J. D. Budai, *Solid-State Electron.* **47**, 2215 (2003).

¹⁷S. Ishizuka, T. Maruyama, and K. Akimoto, *Jpn. J. Appl. Phys., Part 2* **39**, L786 (2000).

¹⁸K. Matsuzaki, K. Nomura, H. Yanagi, T. Kamiya, M. Hirano, and H. Hosono, *Appl. Phys. Lett.* **93**, 202107 (2008).

¹⁹ITO/ATO-coated substrates from Planar Systems, I.E. Finland (2004).

²⁰G. Bernardo, G. Goncalves, P. Barquinha, Q. Ferreira, G. Brotas, L. Pereira, A. Charas, J. Morgado, R. Martins, and E. Fortunato, *Synth. Met.* **159**, 1112 (2009).

²¹E. Fortunato, L. Pereira, P. Barquinha, I. Ferreira, R. Prabakaran, G. Goncalves, A. Goncalves, and R. Martins, *Philos. Mag.* **89**, 2741 (2009).

²²P. Scherrer, *Göttinger Nachrichten Gesell.* **2**, 98 (1918).

²³N. F. Mott, *Rev. Mod. Phys.* **40**, 677 (1968).

²⁴A. Mittiga, F. Biccari, and C. Malerba, *Thin Solid Films* **517**, 2469 (2009).

²⁵M. Tapiero J. P. Zielinge, and C. Noguét, *Phys. Status Solidi A* **12**, 517 (1972).

²⁶T. J. Coutts, D. L. Young, and X. N. Li, *MRS Bull.* **25**, 58 (2000).

²⁷Y. Nakano, S. Saeki, and T. Morikawa, *Appl. Phys. Lett.* **94**, 022111 (2009).